

The Structure Type of Re_2Te_5 , a New $[\text{M}_6\text{X}_{14}]$ Cluster Compound

F. KLAIBER* AND W. PETTER

Institut für Kristallographie und Petrographie, ETH, CH-8092 Zürich, Switzerland

AND F. HULLIGER

Laboratorium für Festkörperphysik, ETH, CH-8093 Zürich, Switzerland

Received July 6, 1982

Re_2Te_5 crystallizes in a new structure type, having space group $Pbca$ (No. 61) with $a = 13.003(5)$, $b = 12.935(7)$, $c = 14.212(5)$ Å, $Z = 12$. All atoms are in the general positions $8(c)$, apart from one Te atom which occupies the special position $4(a)$ in a center of symmetry. The Re atoms are arranged in octahedral $[\text{Re}_6]$ clusters and all the atoms in general positions can be grouped as $\{[\text{Re}_6\text{Te}_8]\text{Te}_6\}$ complexes. The centers of these units and the Te atom in $4(a)$ are arranged like a slightly distorted rock salt structure. The Te atoms can be replaced by Se atoms up to at least 40%. Re_2Te_5 and $\text{Re}_2\text{Se}_2\text{Te}_3$ reveal a semiconductor-like electric behavior which is accounted for by the chemical bonding.

Introduction

The data published hitherto on the Re-Te system are rather conflicting. The first papers (1, 2) reported the existence of only one intermediate phase with composition ReTe_2 . This stoichiometry was suggested by other rhenium-chalcogen systems where ReS_2 and ReSe_2 are the stable phases. According to Johnston *et al.* (1), ReTe_2 is a p -type semiconductor with a high positive Seebeck coefficient (+490 $\mu\text{V/K}$ at $\sim 300\text{K}$) and a room-temperature resistivity $\rho > 100 \Omega \text{ cm}$. Doping with antimony was found to weaken the compound mechanically and to lower the thermopower to +210 $\mu\text{V/K}$ for a sample of composition $\text{ReTe}_{1.95}\text{Sb}_{0.95}$ (1). Furuseth

and Kjekshus (2) found no indication of a range of homogeneity for ReTe_2 . They obtained rhenium telluride single crystals of irregular polyhedral shape by means of chemical transport reactions using iodine as a transport agent. Based on Weissenberg and precession photographs they proposed $Pna2_1$, $Pbca$, or $Pnma$ as possible space groups. From a Guinier photograph they calculated an orthorhombic cell with $a = 12.987(7)$, $b = 13.055(6)$, $c = 14.271(8)$ Å. The pycnometric density was given as 8.50 g/cm^3 as compared to a calculated X-ray density of 8.48 g/cm^3 when assuming $Z = 28$. ReTe_2 was found to be weakly paramagnetic between 100 and 450K, then changing to diamagnetic with a linear decrease up to $-0.05 \times 10^{-6} \text{ emu/g}$ at 730K.

On heating mixtures of Re and Te in various proportions at temperatures between 450 and 935°C Sorrell (3) observed the for-

*Present address: Institut für Angewandte Physik, ETH, CH-8093 Zürich, Switzerland.

mation of a single binary phase of composition ReTe_2 , which he described as being black, of dull sheen, brittle, and soft. Sorrell assigned to the first three lines of the powder diagram the indices (100), (010), and (001) and in this way indexed the powder diagram of his ReTe_2 sample in the triclinic system with the unrealistic cell dimensions $a = 8.992$, $b = 7.520$, $c = 6.882$ Å, $\alpha = 99^\circ 52'$, $\beta = 101^\circ 00'$, $\gamma = 99^\circ 40'$. In fact these lines correspond to (111), (002), and (020) of the orthorhombic cell: Sorrell's powder diagram becomes fairly similar to that listed by Furuseth and Kjekshus (2) when $\Delta\theta = 0.05^\circ$ are added to all his diffraction angles. Sorrell found ReTe_2 (in sealed silica tubes of unknown Te vapor pressure) to melt peritectically to a mixture of solid Re and liquid Te. The mixture was said to be quenchable by rapid cooling. Cooling at a rate of $1^\circ\text{C}/\text{min}$ allows ReTe_2 to form by solid-liquid reaction below 935°C . No ternary compound was observed in the system Pb-Re-Te between 450 and 600°C (1).

Opalovskii *et al.* (4) used the lattice parameters of Furuseth and Kjekshus (2) to index the powder pattern of a rhenium telluride sample which, according to chemical analysis, had the composition $\text{ReTe}_{2.03}$. However, they mentioned that in certain cases weak reflections of metallic rhenium were present, from which we conclude that the true Te:Re ratio of the telluride phase was >2 . In a subsequent paper Opalovskii *et al.* (5) identified the single-phase rhenium telluride as Re_2Te_5 (which was obtained either via the gaseous phase starting with a Re:Te ratio of 1:3 or via a liquid phase of composition Re:Te = 1:6). Wildervanck and Jellinek (6, 7) prepared single crystals of ReTe_2 by iodine transport in a gradient of $980 \rightarrow 840^\circ\text{C}$. Crystals were obtained in the form of brittle blocks with many crystal faces. From Weissenberg diagrams they deduced the space group $Pcab$. Their unit-cell dimensions ($a = 12.972(2)$, $b = 13.060(5)$, $c = 14.254(2)$ Å (6)) are practi-

cally identical with those of Furuseth and Kjekshus (2). A comparison of the molar volumes of MoTe_2 , WTe_2 , TcTe_2 , and ReTe_2 led Wildervanck and Jellinek to assume $Z = 32$ with the consequence of a rather high X-ray density of 9.71 g/cm^3 . DTA experiments showed ReTe_2 (in sealed ampoules) to decompose into the elements at about 975°C . The subsequent recombination of the elements at lower temperatures seemed to be very incomplete, as was concluded from the large amounts of Te present after slowly cooling the DTA ampoule.

Phases of various other compositions were claimed to exist, based on phase analyses of the system Re-Te. Thus Ermolaev and Gukova (8) reported Re_2Te_7 with a congruent melting point of 1000°C , as well as Re_2Te_5 , decomposing peritectically at 968°C . Opalovskii *et al.* (9) claimed to have isolated Re_3Te_2 by reducing $\text{Re}_3\text{Te}_2\text{Cl}_5$ and $\text{Re}_3\text{Te}_2\text{Br}_5$ with hydrogen gas. A single-phase homogeneity region from 68.35 to 72.3% Te (i.e., $\text{ReTe}_{2.16}$ to $\text{ReTe}_{2.61}$) was reported by Yanaki *et al.* (10). Samples with less Te were found to contain free Re. From the given diagram of lattice constants vs concentration we would rather set the lower phase boundary at 67 at% Te. It may be noteworthy that these lattice constants, which increase with Te content, are distinctly larger than any literature values. By reacting H_2Te with either Re powder or NH_4ReO_4 the same authors (11) obtained a broad spectrum of stoichiometries ReTe_x : $x = 1.04, 1.446, 1.84, 2.39, 2.457, 2.475$ with Re, and $x = 1.36, 1.9, 2.16, 2.41, 2.475$ with the perrhenate. For these compositions the electrical resistivity was metallic in character.

From thermal and X-ray diffraction analysis and measurements of microhardness, density, electrical resistivity, and thermopower, Kurbanov *et al.* (12) constructed a phase diagram which shows three phases: a line phase, Re_2Te , with a peritectic temper-

ature of 850°C, and two congruently melting phases with homogeneity regions. Re_2Te had already been reported by Montignie (13). The two alloy-like phases cover the ranges 45 to 52 and 66.6 to 72 at% Te, and have melting points of 900 and 970°C, respectively. The latter phase corresponds roughly to a solution $\text{ReTe}_2\text{-Re}_2\text{Te}_5$. The X-ray diffraction patterns given for ReTe_2 and Re_2Te_5 are similar to those of the other authors. Surprisingly, however, there exist some slight differences between a cast ReTe_2 sample and one which after melting was annealed ten days at 350°C—e.g., a distinct shift of the (002) line. And while the (002) and the (200)/(020) lines of annealed ReTe_2 and Re_2Te_5 coincide, the (111) line of Re_2Te_5 is considerably shifted to higher angles. The thermopower vs composition curve shows a clear maximum for $\text{ReTe}_2\text{-Re}_2\text{Te}_5$, the values for both compositions lying above +500 $\mu\text{V/K}$. Both the resistivity and the density vs composition curves peak near $\text{Re}_2\text{Te}_{4.5}$, the peak values being $\sim 5 \Omega \text{ cm}^{-1}$ and $\sim 11 \text{ g/cm}^3$ (!), respectively. It was stated that the temperature dependence of the electrical resistivity and thermopower revealed *p*-type semiconductivity for ReTe_2 and Re_2Te_5 , as well as for $\text{Re}_{55}\text{Te}_{45}$.

At temperatures above 600°C and at a pressure of 90 kbar, Larchev and Popova (14) obtained a ReTe_2 modification which is isostructural with ReSe_2 : $a = 7.180$, $b = 6.548$, $c = 7.512 \text{ \AA}$, $\alpha = 112.45^\circ$, $\beta = 87.56^\circ$, $\gamma = 120.17^\circ$; $Z = 4$. The pycnometric density was determined to be $10.3(1) \text{ g/cm}^3$, compared with $d_x = 10.57 \text{ g/cm}^3$. No transition to the superconducting state was detected down to 1.7K, and in fact we rather expect nonmetallic properties for ReSe_2 -type ReTe_2 , since the energy gaps for ReS_2 and ReSe_2 (1.33 and 1.15 eV, respectively (7)) are fairly high.

On the basis of all this (mainly inconsistent) information it was at least evident that Re–Re bonds had to be expected in the

structure of the orthorhombic rhenium telluride.

Experimental

Single crystals of rhenium telluride were grown by an iodine transport reaction. The lustrous crystals of up to 1 mm size had obviously the same polyhedral shape as those obtained by Furuseth and Kjekshus (2) and by Wildervanck and Jellinek (6, 7). They also showed the same Seebeck coefficient as reported by Johnston *et al.* (1). The pycnometric density of the small crystals was roughly measured in water, ethanol, and octane to lie between 8 and 9 g/cm^3 . Precession photographs yielded an orthorhombic cell in space group *Pbca* with virtually the same cell dimensions as had been reported for ReTe_2 (2, 6, 7). Electron-beam microanalyses carried out on two crystals, however, revealed the stoichiometry to be close to Re_2Te_5 ($\text{ReTe}_{2.46}$, $\text{ReTe}_{2.51}$). Since in space group *Pbca* the lowest multiplicity of the atomic positions is 4, necessarily $Z = 4n$. In our case $Z = 12$ is the only possibility. This corresponds to an X-ray density of $d_x = 8.42 \text{ g/cm}^3$.

The crystal used for the data collection was ground to a sphere of 0.14 mm diameter. The measurements were carried out on a SYNTEX P2₁ automatic four-circle diffractometer with $\text{MoK}\alpha$ radiation from a graphite monochromator in perpendicular setting. The scan velocity of the $2\theta/\omega$ scan was kept constant at 2°/min within the range $0^\circ < 2\theta \leq 60^\circ$. A total of 4797 reflections were registered of which 2185 were symmetrically independent, 476 of these with $I < 3\sigma(I)$ were marked as “unobserved.” The intensities were corrected for absorption ($\mu = 506 \text{ cm}^{-1}$) by the program CAMEL JOCKEY (15) using 776 ψ -scan measurements of 24 selected reflections from the entire 2θ range. The structure was solved by direct methods with the programs SINGEN and PHASE of the “X-Ray Sys-

TABLE I
LIST OF ATOMIC PARAMETERS

Atom	<i>x</i>	<i>y</i>	<i>z</i>	U_{11}	U_{22}	U_{33}	U_{12}	U_{13}	U_{23}
Re(1)	0.1343(1)	0.4939(1)	0.0511(1)	0.0187(8)	0.0181(6)	0.0151(6)	0.0000(7)	-0.0007(6)	-0.0001(5)
Re(2)	0.0482(1)	0.0589(1)	0.3866(1)	0.0200(8)	0.0181(6)	0.0134(5)	0.0002(6)	0.0003(6)	0.0004(5)
Re(3)	0.4721(1)	0.3666(1)	0.4515(1)	0.0204(8)	0.0169(6)	0.0148(6)	0.0001(7)	0.0004(7)	-0.0007(5)
Te(1)	0.3218(2)	0.4617(2)	0.1276(2)	0.020(1)	0.028(1)	0.021(1)	0.000(1)	-0.002(1)	0.001(1)
Te(2)	0.1155(2)	0.1427(2)	0.2235(1)	0.027(1)	0.022(1)	0.0186(9)	0.000(1)	0.002(1)	0.0024(8)
Te(3)	0.4276(2)	0.1773(2)	0.3783(2)	0.028(1)	0.021(1)	0.020(1)	0.000(1)	0.000(1)	-0.0015(9)
Te(4)	0.2875(2)	0.4336(2)	0.3895(1)	0.020(1)	0.026(1)	0.018(1)	-0.003(1)	-0.002(1)	-0.0018(9)
Te(5)	0.3860(2)	0.1870(2)	0.1165(1)	0.025(1)	0.019(1)	0.018(1)	0.002(1)	0.001(1)	-0.0014(9)
Te(6)	0.0578(2)	0.4195(2)	0.2144(1)	0.025(1)	0.023(1)	0.0157(8)	0.001(1)	-0.001(1)	0.0015(8)
Te(7)	0.1555(2)	0.2013(2)	0.4846(1)	0.024(1)	0.022(1)	0.0207(9)	-0.004(1)	0.000(1)	0.0011(1)
Te(8)	0.0	0.0	0.0	0.029(2)	0.027(2)	0.024(2)	-0.003(2)	0.000(2)	-0.002(1)

Note. The temperature factor has the form of $\exp(-T)$, where $T = 2*(PI**2)*SUMIJ(H(I)*H(J)*U(I,J)*ASTAR(I)*ASTAR(J)$ for anisotropic atoms. $ASTAR(I)$ are reciprocal axial lengths and $H(I)$ are Miller indices. The ESD of the last significant digit is given in parentheses.

tem 72'' (16) and again by MULTAN (17). The three Re atoms and seven Te atoms occupy the general position 8(c) of $Pbca$ and one Te atom is in the center of symmetry in 4(a). Least-squares refinements with anisotropic temperature parameters converged at $R = 0.045$. The corresponding difference map was still uneven but showed only insignificant fluctuations with $\Delta\rho < 3e/\text{\AA}^3$. The atomic and thermal parameters are listed in Table I.¹

The lattice constants were taken from a completely indexed high-precision Guinier photograph with $\text{CuK}\alpha_1$ radiation and silicon ($a_{295\text{K}} = 5.43054 \text{\AA}$) as a standard. A least-squares refinement resulted in $a = 13.003(5)$, $b = 12.935(7)$, $c = 14.212(5) \text{\AA}$ with orthorhombic constraints. From this we calculated the interatomic distances given in Table II.

Discussion of the Re_2Te_5 Structure

The most striking feature of the Re_2Te_5 structure is the Re-Re bonding. All Re atoms are arranged in discrete $[\text{Re}_6]$ clusters. The bond distances within these clusters

are comparable with those of the $[\text{Re}_6]$ clusters in $\text{Na}_2\text{Re}_3\text{S}_6$: 2.593 to 2.619 \AA (18), $\text{K}_2\text{Re}_3\text{S}_6$: 2.610 to 2.635 \AA (18), $\text{Cs}_4\text{Re}_6\text{S}_{13}$: 2.61 \AA (19), and with the shortest Re-Re distance found in ReSe_2 : 2.65, 2.84, 2.93, and 3.08 \AA (20), as well as with the Mo-Mo distances in the "nonmetallic" endmember $\text{M}_2^+\text{Mo}_6\text{S}_8$: 2.66 to 2.68 \AA (21, 22) and in MoCl_2 : 2.61 \AA (23). A similar arrangement of the Re atoms is met in $\text{Sr}_2\text{Re}_6\text{S}_{11}$ and $\text{Ba}_2\text{Re}_6\text{S}_{11}$ (24) and in the Chevrel phases $\text{Mo}_2\text{Re}_4\text{S}_8$ and $\text{Mo}_2\text{Re}_4\text{Se}_8$ (25). The near-neighbor coordination of the metal atoms is in fact identical in these compounds: In Re_2Te_5 eight Te atoms, here named Te(4) to Te(7), are arranged above the triangular octahedron faces, and they surround the $[\text{Re}_6]$ octahedron in the form of a cube resulting in an $[\text{M}_6\text{X}_8]$ cluster of the same shape as the anions in the Chevrel phases. Only the relative orientation of the $[\text{M}_6\text{X}_8]$ unit differs. The $[\text{Re}_6\text{Te}_8]$ partial structure of Re_2Te_5 is represented in Fig. 1. The $[\text{Re}_6\text{Te}_8]$ units themselves are connected with each other via almost planar butterfly-like $[\text{Te}(8)\{\text{Te}(1) \text{Te}(2) \text{Te}(3)\}_2]$ units as shown in Figs. 2 and 3. The Te(1), Te(2), and Te(3) atoms are each connected with one Re atom as well as with two Te atoms, but the coordinations are not equivalent.

¹ A list of structure factors can be obtained from the first author.

TABLE II
 INTERATOMIc DISTANCES IN Re_2Te_5

Re(1)–Re(2)	2.667(3)	Re(2)–Re(1)	2.667(2)	Re(3)–Re(1)	2.678(2)
Re(2)	2.681(2)	Re(1)	2.681(2)	Re(1)	2.675(2)
Re(3)	2.678(2)	Re(3)	2.682(2)	Re(2)	2.682(2)
Re(3)	2.675(2)	Re(3)	2.667(2)	Re(2)	2.667(2)
Te(4)	2.681(3)	Te(4)	2.682(3)	Te(4)	2.700(3)
Te(5)	2.678(3)	Te(5)	2.681(3)	Te(5)	2.688(3)
Te(6)	2.701(3)	Te(6)	2.686(3)	Te(6)	2.696(3)
Te(7)	2.709(3)	Te(7)	2.698(3)	Te(7)	2.698(3)
Te(1)	2.701(3)	Te(2)	2.704(2)	Te(3)	2.723(3)
Re(1)	3.785(3)	Re(2)	3.779(2)	Re(3)	3.786(3)
Te(1)–Re(1)	2.701(3)	Te(2)–Re(2)	2.704(3)	Te(3)–Re(3)	2.723(3)
Te(2)	2.828(3)	Te(1)	2.828(3)	Te(2)	2.874(4)
Te(8)	2.983(3)	Te(3)	2.874(4)	Te(8)	3.022(3)
Te(7)	3.639(4)	Te(6)	3.660(4)	Te(5)	3.762(3)
Te(4)–Re(1)	2.681(3)	Te(5)–Re(1)	2.678(3)	Te(6)–Re(1)	2.701(3)
Re(2)	2.682(3)	Re(2)	2.681(3)	Re(2)	2.686(3)
Re(3)	2.700(3)	Re(3)	2.688(3)	Re(3)	2.696(3)
Te(7)	3.715(4)	Te(1)	3.653(4)	Te(2)	3.660(4)
Te(7)–Re(1)	2.709(3)	Te(8)–2Te(1)	2.983(3)		
Re(2)	2.698(3)	2Te(3)	3.022(3)		
Re(3)	2.698(3)	2Te(2)	3.968(2)		
Te(1)	3.639(4)				

Note. Distances (in Å) up to the closest nonbonding contact are listed. Standard deviations are in parentheses.

As can be seen from Figs. 2 and 3, Te(1), Te(2), and Te(3) define a large octahedron surrounding the $[\text{Re}_6\text{Te}_8]$ cluster in such a way that each of these Te atoms neighbors

the Re atom with equal numbering. Therefore we end up with $\{[\text{Re}_6\text{Te}_8]\text{Te}_6\}$ units containing a center of symmetry in the unoccupied 4(b) position. Thus these $\{[\text{Re}_6$

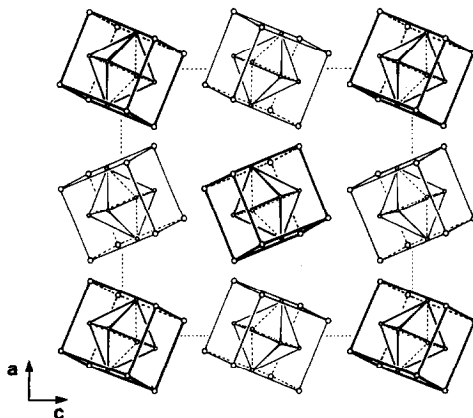


FIG. 1. Projection of the $[\text{Re}_6\text{Te}_8]$ partial structure of $\text{Re}_2\text{Te}_5 = \{[\text{Re}_6\text{Te}_8]\text{Te}_6\}\text{Te}$. Geometrical description as $[\text{Re}_6]$ octahedra inside $[\text{Te}_8]$ cubes.

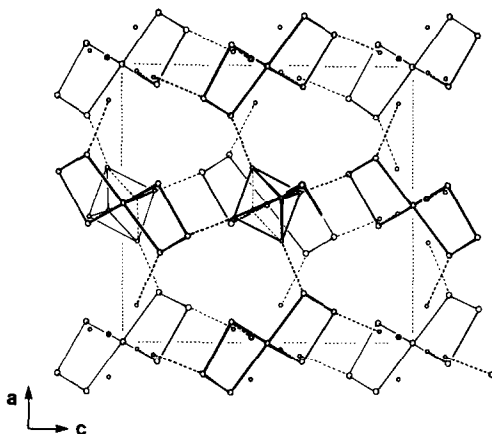


FIG. 2. $\{[\text{Te}_6]\text{Te}\}$ partial structure of $\text{Re}_2\text{Te}_5 = \{[\text{Re}_6\text{Te}_8]\text{Te}_6\}\text{Te}$. The bonding within the butterfly-like Te units is visualized by full lines. Broken lines indicate Re-Te bonds connecting the $[\text{Re}_6]$ octahedra (two of which are added in the middle part of the figure) via the wings of the butterfly units. The apices of the chemically meaningless large $[\text{Te}_6]$ octahedra (i.e., the terminal Te atoms at the broken lines) form part of six different butterfly units, and vice versa, the atoms defining the wings of the butterfly units belong to six different $\{[\text{Te}_6]\text{Te}\}$ octahedra.

$\text{Te}_8/\text{Te}_6\}$ clusters, together with the Te(8) atoms in 4(a), form an orthorhombically distorted rock salt structure. A similar rock salt derivative is met in the cubic structure of $\text{HgMo}_6\text{Cl}_{14} = \text{Hg}\{[\text{Mo}_6\text{Cl}_8]\text{Cl}_6\}$ (26). For comparison we may note that the Pb atoms and the $[\text{Mo}_6\text{S}_8]$ clusters in the Chevrel phase PbMo_6S_8 occupy the positions of a rhombohedrally deformed CsCl structure.

The $[\text{Mo}_6\text{Cl}_8]^{4+}$ unit in $\text{MoCl}_2 = [\text{Mo}_6\text{Cl}_8]\text{Cl}_4$ is obviously equivalent to a

$[\text{Re}_6\text{Te}_8]^{2+}$ unit. Furthermore, the $\{[\text{Re}_6\text{Te}_8]\text{Te}_6\}$ unit of Re_2Te_5 is reminiscent of the cluster ions $\{[\text{Mo}_6\text{Cl}_8]\text{Cl}_6\}^{2-}$ and $\{[\text{Mo}_6\text{Cl}_8]\text{Br}_6\}^{2-}$ as well as of $\{[\text{Re}_6\text{S}_8]\text{S}_{2/2}(\text{S}_2)_{3/2}\}^{4-}$ met in $\text{Cs}_4\text{Re}_6\text{S}_{13}$ (19) and of $\{[\text{Re}_6\text{S}_8]\text{S}_{4/2}(\text{S}_2)_{2/2}\}^{4-}$ met in $\text{K}_2\text{Re}_3\text{S}_6$ (18). In the $[\text{Re}_6]$ octahedron 24 d electrons are used for the intracuster bonding while 30 d,p,s orbitals (dsp^3 hybrids) and 18 valence electrons are available for Re-Te bonding. The $[\text{Te}_6]$ unit offers 24 p orbitals

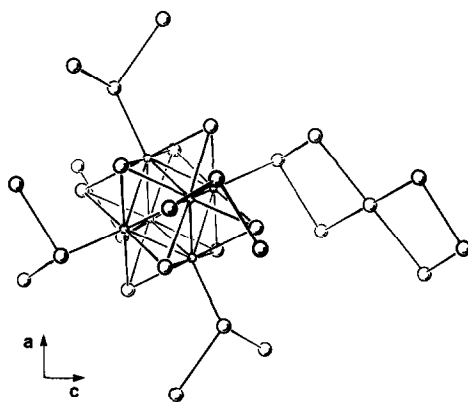


FIG. 3. Chemical bonds around an $[\text{Re}_6]$ octahedron of the Re_2Te_5 structure. Large spheres: Te; small spheres: Re.

and 32 electrons for Te–Re bonding, which means that a total of 50 electrons has to be distributed into 24 orbitals. Thus we are left with two excess electrons (therefore giving $[\text{Re}_6\text{Te}_8]^{2+}$) and one orbital per Re atom for binding the outer Te atoms. The butterfly-like $\{\text{Te}[\text{Te}_6]\}$ unit requires electrons for six Te–Re bonds and eight Te–Te bonds. If we want to attain bond saturation to account for the nonmetallic behavior then these 14 bonds require 28 of the available 30 valence electrons (2 from the $[\text{Re}_6\text{Te}_8]$ cluster and $7 \times 4 p$ electrons from the Te atoms). This leads to an uncommon configuration of Te(8) with four bonding orbitals and two nonbonding inert pairs. Formally, the extreme covalent charge distribution can be described by a formula $\{[\text{Re}_6^{2-}\text{Te}_8^+]\text{Te}_6^+\}$ “ Te^{2-} ”, while the extreme ionic description would correspond to $\{[\text{Re}_6^{3+}\text{Te}_8^{2-}]\text{Te}_6^0\}$ “ Te^{2-} ”. The quotation marks in these formulas should indicate that “ Te^{2-} ” is a rather uncommon “anion.” In fact, Te(8) in position 4(a) has a nonxenon-like electron configuration: In addition to the 5s and the three 5p wavefunctions, two 5d wavefunctions are involved in the formation of the valence band. This is reflected in the larger distances. Although nonmetallic, Re_2Te_5 therefore cannot be a Mooser–Pearson phase where only s and p wavefunctions of the anions are allowed. The electronic configuration of $\text{Te}(8)^{2-}$ corresponds to that of xenon in the square-planar XeF_4 unit and to that of iodine in the anion ICl_4^- . An identical coordination of Te with similar distances is met in the tetragonal structure of Ga_2Te_5 (27), where infinite tetrahedron chains $[\text{GeTe}_{4/2}]_\infty$ are linked by four-coordinated d-bonding Te atoms. Further examples are offered by the structures of Cs_2Te_5 (28) and K_2SnTe_5 (31), which are governed by a similar building principle.

The Re_2Te_5 type of structure might be appropriate for a nonmetallic ternary phase $\{[\text{Re}_6\text{Te}_8]\text{Te}_6\}\text{Pd}$ with “divalent” palladium. If, on the other hand, we put Re at the place

of Te(8) in 4(a) a metallic compound $\{[\text{Re}_6\text{Te}_8]\text{Te}_6\}\text{Re}$ of the exact composition ReTe_2 would result. This was checked here and is definitely not the case.

Substitutions and Possible Insertions

A compound with 2 : 5 stoichiometry has been reported in the system Re–S (29). Re_2S_5 has a definitely different structure according to the published powder diagram which has been indexed based on an orthorhombic cell with $a = 4.806$, $b = 5.667$, $c = 4.75$ Å. A similar selenide apparently does not exist. We prepared mixed phases $\text{Re}_2(\text{Te}_{1-x}\text{Se}_x)_5$ by sintering pressed elemental powders at 600 to 850°C. For values $x \geq 0.5$ we invariably detected ReSe_2 as a second phase even after repeated regrinding and reheating. The Guinier pattern of $\text{Re}_2\text{Se}_2\text{Te}_3$ was indexed and the following lattice constants were calculated as $a = 12.695(6)$, $b = 12.653(5)$, $c = 14.143(5)$ Å. This particular stoichiometry seemed to favour a certain anion ordering. With the aid of LAZY PULVERIX (30) we calculated intensities for three possible types of ordering: $\text{Re}_2(\text{Se}_{0.4}\text{Te}_{0.6})_5$ with statistical distribution, $\{[\text{Re}_6(\text{Se}_{0.75}\text{Te}_{0.25})_8]\text{Te}_6\}\text{Te}$, and $\{[\text{Re}_6\text{Te}_8]\text{Se}_6\}\text{Te}$, assuming the site parameters of Re_2Te_5 to be valid in a first approximation. The last case, which appeared to be most likely from a “mathematical” point of view, could definitely be ruled out. The second case is favored with respect to the first case, but the differences are less pronounced, based mainly on two weak lines. The model with the Se atoms located on the cube around the $[\text{Re}_6]$ octahedron (ordered or disordered) is, however, supported by the fact that the c axis contracts much less than the a and b axes (see Fig. 2). However, our attempts to occupy all the cube positions by Se atoms failed.

Doping with Sb is obviously possible to a fairly high degree (1). This behavior is rather strange for a semiconductor and, in

fact, we would expect a simultaneous substitution of the metal atoms to be necessary, e.g., $\text{Ru}_2\text{Sb}_2\text{Te}_3$, but we failed to synthesize this hypothetical isotype. Superimposing Figs. 1 and 2 shows that the Re_2Te_5 structure contains rather large voids. Thus an 8(c) site with $x = 0.2801$, $y = 0.2694$, $z = 0.2659$ (center of the void) has the following neighborhood:

center—

Te(2), Te(3), Te(4), Te(5) at 2.754(7) Å,
Te(1) at 3.213(6) Å,
Te(6) at 3.566(7) Å,
Te(7) at 3.617(6) Å.

This void in $\text{Re}_6\Box_2\text{Te}_{15}$ is obviously large enough to take up an additional metal atom: $\text{Re}_6M_2\text{Te}_{15}$ (e.g., $M = \text{Ag}, \text{Cd}, \text{In}, \dots$).

Electrical Resistivity

In order to check the reported semiconductivity we measured the electrical resistivity from room temperature up to $\sim 1000\text{K}$ on a sintered Re_2Te_5 sample and on a Re_2Te_5 single crystal, as well as on a sintered $\text{Re}_2\text{Se}_2\text{Te}_3$ sample. In all these cases we observed a semiconductor behavior with activation energies E_g between 0.6 and 0.8 eV, assuming $\rho \sim \exp(-E_g/2kT)$. Room-temperature resistivities were $\sim 1000 \Omega \text{ cm}$. Repeated heating cycles in a vacuum of 10^{-5} mm Hg lowered the resistivity of the sintered samples, possibly due to some evaporation of Te.

Acknowledgments

The authors are indebted to Miss Lotti Keller for technical assistance, as well as to Mr. Roman Gubser for the electron beam microanalysis. F.H. thanks Dr. Wolfgang Hönl, MPI Stuttgart, for Ref. (28) and for a discussion on the bonding. This work was supported by the Swiss National Science Foundation.

References

1. W. D. JOHNSTON, R. C. MILLER, AND D. H. DAMON, *J. Less-Common Met.* **8**, 272 (1965).
2. S. FURUSETH AND A. KJEKSHUS, *Acta Chem. Scand.* **20**, 245 (1966).
3. C. A. SORRELL, *J. Amer. Ceram. Soc.* **51**, 285 (1968).
4. A. A. OPALOVSKII, V. E. FEDOROV, E. U. LOBKOV, B. G. ÉRENBURG, AND L. N. SENCHENKO, *Izv. Akad. Nauk SSSR Neorg. Mater.* **6**, 561 (1970); *Inorg. Mater.* **6**, 495 (1970).
5. A. A. OPALOVSKII, V. E. FEDOROV, B. G. ÉRENBURG, E. U. LOBKOV, YA. V. VASIL'EV, L. N. SENCHENKO, AND B. I. TSIKANOVSKII, *Zh. Fiz. Khim.* **45**, 2110 (1971); *Russ. J. Phys. Chem.* **45**, 1197 (1971).
6. J. C. WILDERVANCK, Doctoral thesis, University of Groningen NL (1970).
7. J. C. WILDERVANCK AND F. JELLINEK, *J. Less-Common Met.* **24**, 73 (1971).
8. M. I. ERMOLAEV AND YU. YA. GUKOVA, "Issled. Primen. Splavov Reniya, Dokl. Vses. Soveshch. Probl. Reniya, 4th, 1973," (E. M. Savitskii and M. A. Tylkina, Eds.), p. 74, "Nauka", Moscow (1973); *Chem. Abstr.* **84**, 93'789m (1976).
9. A. A. OPALOVSKII, V. E. FEDOROV, AND E. U. LOBKOV, *Izv. Sib. Otd. Akad. Nauk SSSR Ser. Khim. Nauk* 144 (1971); *Chem. Abstr.* **76**, 53'827a (1972).
10. A. A. YANAKI, V. A. OBOLONCHIK, AND R. V. SKOLOZDRA, *Izv. Akad. Nauk SSSR Neorg. Mater.* **7**, 862 (1971); *Inorg. Mater.* **7**, 755 (1971).
11. V. A. OBOLONCHIK AND A. A. YANAKI, "Tr. Vses. Soveshch. Probl. Reniya, 3rd, 1968" (E. M. Savitskii, Ed.), Nauka, Moscow (1970); *Chem. Abstr.* **74**, 131'004e (1971).
12. T. KH. KURBANOV, R. A. DOVLYATSHINA, I. A. DZHAVADOVA, AND F. A. AKHMEDOV, *Zh. Neorg. Khim.* **22**, 1137 (1977); *Russ. J. Inorg. Chem.* **22**, 622 (1977).
13. E. MONTIGNIE, *Z. Anorg. Allg. Chem.* **366**, 111 (1969).
14. V. I. LARCHEV AND S. V. POPOVA, *Izv. Akad. Nauk SSSR Neorg. Mater.* **12**, 1365 (1976); *Inorg. Mater.* **12**, 1130 (1976).
15. H. D. FLACK, *Acta Crystallogr. Sect. A* **33**, 890 (1977).
16. "THE X-RAY SYSTEM 72," Technical Report TR-192, Computer Science Center, Univ. of Maryland, College Park (1972).
17. P. MAIN *et al.*, "MULTAN 77, a System of Computer Programs for the Automatic Solution of Crystal Structures from X-Ray Diffraction Data," (1977). Available from Department of Physics, Univ. of York, England.
18. W. BRONGER AND M. SPANGENBERG, *J. Less-Common Met.* **76**, 73 (1980).
19. M. SPANGENBERG AND W. BRONGER, *Angew. Chem. Int. Ed. Engl.* **17**, 368 (1978).

20. N. W. ALCOCK AND A. KJEKSHUS, *Acta Chem. Scand.* **19**, 79 (1965).
21. K. YVON AND A. PAOLI, *Solid State Commun.* **24**, 41 (1977).
22. K. YVON, in "Current Topics in Materials Science" (E. Kaldis, Ed.), Vol. 3, p. 54, North-Holland Amsterdam (1979).
23. H. SCHÄFER, H. G. v. SCHNERING, J. TILLAK, F. KUHNEN, H. WÖHRLE, AND H. BAUMANN, *Z. Anorg. Allg. Chem.* **353**, 281 (1967).
24. W. BRONGER AND H. J. MIESSEN, *J. Less-Common Met.* **83**, 29 (1982).
25. A. PERRIN, M. SERGENT, AND O. FISCHER, *Mater. Res. Bull.* **13**, 259 (1978).
26. H. G. v. SCHNERING, *Z. Anorg. Allg. Chem.* **385**, 75 (1971).
27. M. JULIEN-POUZOL, S. JAULMES, AND F. ALAPINI, *Acta Crystallogr. Sect. B* **33**, 2270 (1977).
28. P. BOETTCHER AND U. KRETSCHMANN, *Z. Anorg. Allg. Chem.* (1982).
29. G. ODENT, *Rev. Chim. Minér.* **8**, 145 (1977).
30. K. YVON, W. JEITSCHKO, AND E. PARTHÉ, *J. Appl. Crystallogr.* **10**, 73 (1977).
31. B. EISENMANN, H. SCHWERER, AND H. SCHÄFER, *Mater. Res. Bull.* **17** (1982).